Postprint:
Zhongde Dai, et al., Industrial & Engineering Chemistry Research, 2022, 61, 25, 9067–9076
https://doi.org/10.1021/acs.iecr.2c01402

Nanocellulose crystals enhanced hybrid membrane for CO_2 capture

Zhongde Dai[1,2,3,4*], Jing Deng[5*], Yulei Ma[1,2,3,4], Hongfang Guo[1,2,3,4], Jing Wei[1,2,3,4],

Bangda Wang[1,2,3,4], Xia Jiang[1,2,3,4], Liyuan Deng[6*]

[1]College of Architecture and Environment, Sichuan University, Chengdu 610065, China

[2]National Engineering Research Centre for Flue Gas Desulfurization, Sichuan University, Chengdu, Sichuan, 610065, China

[3]Carbon Neutral Technology Innovation Center of Sichuan, Sichuan University, Chengdu, Sichuan, 610065, China

[4]School of Carbon Neutrality Future Technology, Sichuan University, Chengdu, Sichuan, 610065, China

[5]School of Chemical, Biological and Materials Engineering, University of Oklahoma, Norman, Oklahoma, 73019, USA

[6]Department of Chemical Engineering, Norwegian University of Science and Technology Trondheim, 7491, Norway

*Corresponding Author:

Zhongde Dai: zhongde.dai@scu.edu.cn,

Jing Deng: Jing.Deng-1@ou.edu

Liyuan Deng: liyuan.deng@ntnu.no

Keywords: hybrid membranes, nanocellulose crystal, Pebax, CO_2 capture

Abstract:

Developing membrane material with both high CO_2 permeability and high CO_2/N_2 selectivity is always desired for CO_2 capture while improving the sustainability of the membrane preparation process is of equal importance. In the current work, nanocellulose crystal (CNC) was blended with hydrophilic Pebax^{TM} 1657 for CO_2 separation application. The CO_2/N_2 separation performance of Pebax 1657/CNC hybrid membranes with up to 40 wt.% CNC was tested by mixed-gas permeation test under both dry and humid conditions. Humid test condition simultaneously increases CO_2 permeability and CO_2/N_2 selectivity of all CNC/Pebax hybrid membranes, compared to those in dry conditions. Introduction of only 5 wt.% CNC into Pebax 1657 realizes 42% and 18% increments in CO_2 permeability (305.7 Barrer) and CO_2/N_2 selectivity (41.6), respectively. However, further increasing CNC loading increases the touristy

of the membrane and results in the self-assembly of CNC in the Pebax matrix, which is observed by SEM, thus leading to both reduced gas permeability and CO_2/N_2 selectivity. The CO_2/N_2 separation results of 5 wt.% CNC/Pebax locates close to Upper Bound 2008, showing its potential as CO_2/N_2 separation membrane materials.

Highlights:

* CNC was blended into Pebax 1657 to improve CO_2 separation performance.

* CNC/Pebax 1657 hybrid membranes with up to 40% CNCs showed no phase separation;

* P(CO_2) and CO_2/N_2 selectivity improved 42% and 18% by adding only 5% CNC in Pebax;

* CO_2 permeability of 305.7 Barrer and CO_2/N_2 selectivity of 41.6 were achieved.

Graphic abstract:

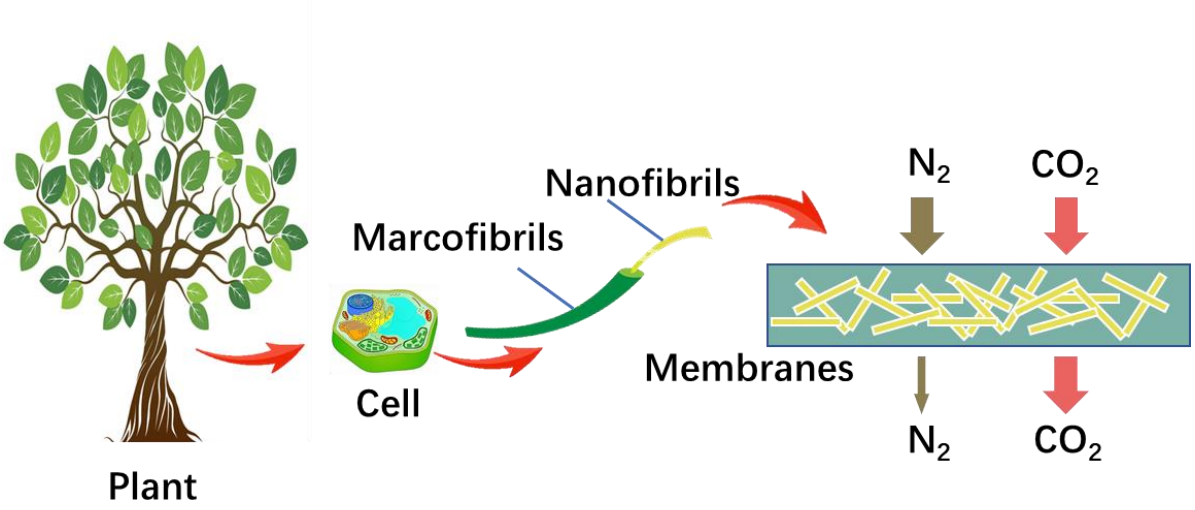

Postprint:
Zhongde Dai, et al., Industrial & Engineering Chemistry Research, 2022, 61, 25, 9067–9076
https://doi.org/10.1021/acs.iecr.2c01402

1. Introduction

Carbon capture, Utilization, and Storage (CCUS) is widely considered as one of the most economical and feasible strategies for effectively curbing greenhouse gas emissions and mitigating climate change.[1, 2] Membrane separation has been believed as an effective approach for post-combustion CO_2 capture accounting for low cost for both operation and maintenance, high separation performance, remarkable energy efficiency, etc.[3, 4] For gas separation membrane technology, the performance of a process is largely dependent on the membrane material.[5] Therefore, materials with improved separation performance can enhance the process efficiency and thus lower the cost.[6-8]

Nanocellulose, as a representative biomaterial, attracted researchers' attention due to its unique properties (e.g., remarkably high mechanical properties, excellent surface area, and a great number of hydroxyl groups available for functionalization).[9, 10] Although nanocellulose is well-known for its gas-barrier property (impermeable for gas & water vapor) due to its crystalline nature,[11] recently researchers have noticed the gas transport in nanocellulose is actually greatly affected by the test conditions and the type of nanocellulose. For example, the CO_2 permeability of self-standing nanocellulose fiber (CNF) membrane is around 0.04 Barrer, at room temperature and dry conditions.[12] However, once the feed is humid, nanocellulose is plasticized by the sorbed water vapor, resulting in orders of magnitude improvement in CO_2 permeability.[13, 14] Ansaloni et al. observed the CO_2 permeability of neat CNF self-standing membrane increases by more than 1000 times when relative humidity (RH) increased from 30% to 85%.[13] More importantly, its ideal CO_2/N_2 selectivity at 85 RH% can reach the order of 500, compared to 30-60 of conventional CO_2 separation membrane materials. These features of nanocellulose, combined with excellent mechanical property, abundance in nature, and low cost, have attracted extensive attention from membrane fields, especially for flue gas purification, where CO_2 needs to be removed from humid feed (mainly N_2).

In flue gas purification, the feed volume needed to be purified is large, which requires a high working capacity of the membrane (i.e., high gas flux). It is even suggested high CO_2 permeability is preferred over high CO_2/N_2 selectivity.[11] Despite the impressive enhancement in gas transport property under humid conditions, the CO_2 permeability of neat nanocellulose is still not high enough. To further raise CO_2 permeability, nanocellulose has been blended with polymers, especially hydrophilic ones. In 2017, Ansaloni et al. fabricated CNF/polyvinylamine (PVAm) hybrid membranes and investigated their gas permeability under different relative humidity conditions.[13] The hybrid material with 50 wt.% CNF exhibits

a CO_2 permeability of 190 Barrer at 90 RH%, compared to 25 Barrer of neat nanocellulose membrane at the same condition. However, the corresponding ideal CO_2/N_2 selectivity drops to around 40. The same research group continued this study by using another kind of nanocellulose (i.e.: nanocellulose crystal, CNC),[14] the length of which is generally one order of magnitude lower than CNF.[15] Under optimized humid conditions (35 ^oC, 90 RH%), the neat CNC membrane has lower CO_2/N_2 and CO_2/CH_4 ideal selectivities (65 and 52, respectively), but a higher CO_2 permeability (i.e., 130 Barrer), compared to that of the neat CNF membrane, due to its less entangled network, resulting from the short length of CNC. Surprisingly, blending with PVAm improved both CO_2 permeability (187 Barrer) and CO_2/N_2 ideal selectivity (100) at 35 ^oC and 80 RH%, when the CNC amount in the membrane is 30 wt.%. The different trends of CNC and CNF-based membrane, after blending with PVAm, may be reasoned by both higher water sorption and lower tortuosity in CNC than in CNF.

Similar results have also been reported by Dai et al.,[16] which employed polyvinyl alcohol (PVA) as the polymer phase instead of PVAm. Similar to the nanocellulose/PVAm membrane, PVA-based hybrid materials containing CNC displayed higher CO_2 permeance than those with CNF. For example, the addition of 80 wt.% CNC into PVA results in a 65% enhancement in CO_2 permeance, while this value for the analog with CNF is only 15%, compared to the neat PVA membrane. Additionally, the kind of nanocellulose has little influence on the CO_2/N_2 selectivity in the PVA/nanocellulose hybrid materials. It is worth mentioning that the 80 wt.% CNC/PVA membrane exhibits excellent long-term stability, which shows no decline in CO_2 permeance and CO_2/N_2 selectivity for more than 1 year. Improved CO_2 separation performance by adding nanocellulose into the PVA phase has been observed and reported by several other authors.[17-20]

From these results, it is clear that blending with hydrophilic polymers and humid permeation tests are of great benefits for nanocellulose-based hybrid membranes. Besides PVA and PVAm, Pebax is also well-known for its hydrophilicity, which has been even employed as natural gas dehydration membrane, because of the high water vapor permeability[21]. Additionally, due to its excellent CO_2 separation performances, it has also been widely accepted in CO_2 separation field[22]. Therefore, to continue these studies, in this work, the potential of Pebax as continues phase for CNC-based hybrid membranes was exposed and reported targeted CO_2/N_2 separation. More specifically, Pebax 1657 was chosen as it is one of most studied Pebax. Various techniques were employed to systematically characterize the obtained CNC/Pebax hybrid membranes. The nanoscale morphology and chemical structure of the CNC/Pebax hybrid

Postprint:
Zhongde Dai, et al., Industrial & Engineering Chemistry Research, 2022, 61, 25, 9067–9076
https://doi.org/10.1021/acs.iecr.2c01402

membrane were evaluated by scanning electron microscope (SEM), and fourier-transform infrared (FTIR), respectively. Both thermogravimetric analysis (TGA) and differential scanning calorimetry (DSC) were employed for studying the hybrid material's thermal properties. While X-ray crystallography was chosen to study the crystalline properties of CNC/Pebax hybrid materials. CO_2/N_2 separation properties of hybrid membrane were thoroughly explored by mixed-gas permeation tests under both dry and humid conditions.

2. Experimental

2.1. Materials

Pebax® MH 1657 (Pebax®1657, consisting of 60 wt.% polyethylene glycol and 40 wt.% polyamide), chemical structure of which is shown in **Figure 1**, was purchased from Arkema Inc. CNC aqueous slurry with a concentration of 12.1 wt. % made from wood pulp was ordered from the University of Maine, USA. Absolute ethanol (EtOH) was obtained from Sigma, Norway. All chemicals were used as received without further purification.

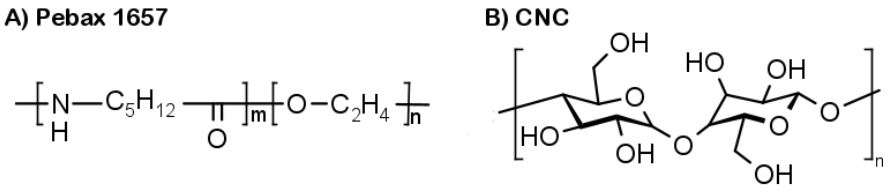

Figure 1. Chemical structure of A) Pebax 1657, and B) CNC

2.2 Membrane preparation

Pebax 1657 was dissolved in the EtOH/water (70/30 wt.%) mixture at 80 °C for around 4 hours with a concentration of 4 wt.%. Then the Pebax solution was mixed with the desired amount of CNC aqueous slurry (12.1 wt.%), and further diluted to a total solid concentration of ca. 2 wt.%. Afterward, the mixture was poured into a Teflon petri dish and dried at 40 °C in a convective oven until a self-standing membrane formed. The thickness of these self-standing membranes is 70-100 μm.

The CNC content (ω_{CNC} , wt%) in membranes was calculated from equation (1):

$$\omega_{CNC} = \frac{w_{CNC}}{w_{CNC}+w_{Pebax}} \times 100 \quad (1)$$

where w_{CNC} and w_{Pebax} are the weights of CNC and Pebax, respectively.

2.3 Characterization

Various characterization techniques have been used to characterize the resultant CNC/Pebax membranes. TGA (TG 209F1 Libra, Netzsch, Germany) and DSC (214 Polyma, Netzsch, Germany) were used to characterize the thermal properties. In the TGA test, approximately 10 mg of sample was heated from room temperature to 800 °C with a rate of 10 °C /min. In the DSC test, around 5 mg of samples were placed in the crucible, with a heating and cooling rate of 10 °C /min in the temperature range between -100 °C to 250 °C. For both TGA and DSC tests, N_2 was employed as both sweep gas and protective gas. A Nicolet iS-50 FTIR spectrometer (Thermo Scientific, USA) equipped with a Specac ATR unit (Golden Gate high performance single reflection monolithic diamond ATR) was chosen to study the chemical structure of the hybrid materials. All FTIR spectra were obtained by averaging 32 scans. Membrane morphology was investigated using an SEM (TM3030 tabletop microscope, Hitachi, Japan). All samples were sputter-coated with gold for around 60 seconds before the SEM test to improve the conductivity. Membrane samples for cross-section were prepared by breaking the membranes in liquid N_2 to preserve the morphology. A D8 A25 DaVinci X-ray Diffractometer (Bruker, Germany) was used to carry out the XRD measurements, which were taken in the 2θ range from 5° to 75° with a step size of 0.045°.

2.4 Gas permeation test

Gas-separation test was conducted using a mixed-gas permeation apparatus, as shown in **Scheme 1**, described in our previous work.[16] Briefly, a CO_2/N_2 (10/90 v/v) gas mixture was employed as the feed gas, whereas pure CH_4 was used as the sweep gas instead of the inert gas Helium since Helium was used as the carrier gas for the gas chromatograph (GC). Humidifiers were equipped for both feed and sweep streams. In both feed and sweep streams, by adjusting the flow ratio between dry and wet streams through mass flow controllers (El-Flow series, Bronkhorst), a desirable humidity can be achieved. The feed pressure was set to ~2 bar using a back-pressure regulator (El-Press series, Bronkhorst) and monitored by a pressure sensor (Wika, S-10). The pressure of the permeate side remained at 1.05 bar, recorded by a pressure sensor mounted on the permeate side. The compositions of retentate and permeate streams were tested by a calibrated gas chromatography (490 Micro GC, Agilent). All tests were conducted at room temperature (R.T.). For each test, at least 6 h is needed to ensure the steady-state was

reached.

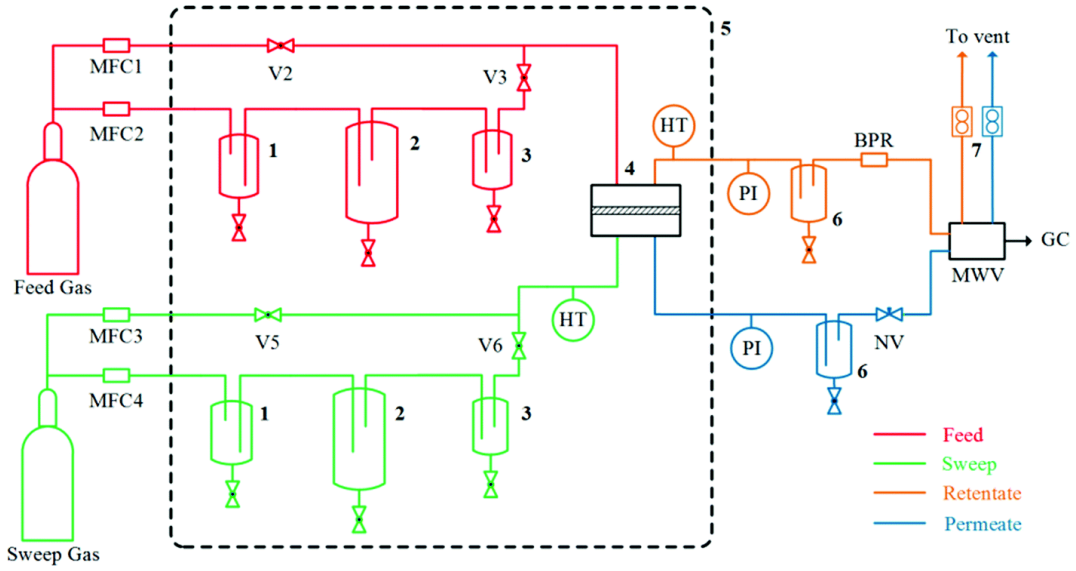

Scheme 1 Mixed-gas permeation apparatus. MCF: mass flow controller; HT: humidity and temperature sensor; PI: pressure indicator; BPR: backup pressure regulator; NV: needle valve; MWV: multiway valve; GC: gas chromatograph; 1: safety trap; 2: humidifier; 3: droplet trap; 4: membrane module; 5: oven; 6; water knockout; 7: bubble flow meters.

The permeability (P_i) of the *i*th penetrant species was calculated by equation (2):

$$P_{m,i} = \frac{N_{perm}(1-y_{H_2O})y_i l}{A(\langle p_{i,feed}, p_{i,ret}\rangle - p_{i,perm})} \quad (2)$$

where N_{perm} is the permeate flow measured with a bubble flow meter, y_{H_2O} is the molar fraction of water in the permeate flow (calculated according to the RH value and the vapor pressure at the given temperature), y_i is the molar fraction of gas *i* in the permeate, and $p_{i,feed}$, $p_{i,ret}$ and $p_{i,perm}$ identify the partial pressures of the *i*th species in the feed, retentate and permeate, respectively. The CO_2/N_2 selectivity is presented by the separation factor ($\alpha_{i/j} = \frac{y_i/x_i}{y_j/x_j}$). It is worth mentioning that for all the gas permeation tests, at least two membrane samples were tested with a standard deviation value lower than 10%, thus the average value was reported without an error bar.

Postprint:
Zhongde Dai, et al., Industrial & Engineering Chemistry Research, 2022, 61, 25, 9067–9076
https://doi.org/10.1021/acs.iecr.2c01402

3. Results and discussion

3.1 Membrane morphology study

To investigate the dispersion of CNC in the Pebax matrix, the morphologies of CNC/Pebax hybrid membranes were investigated by SEM, and the results are shown in **Figure 2**.

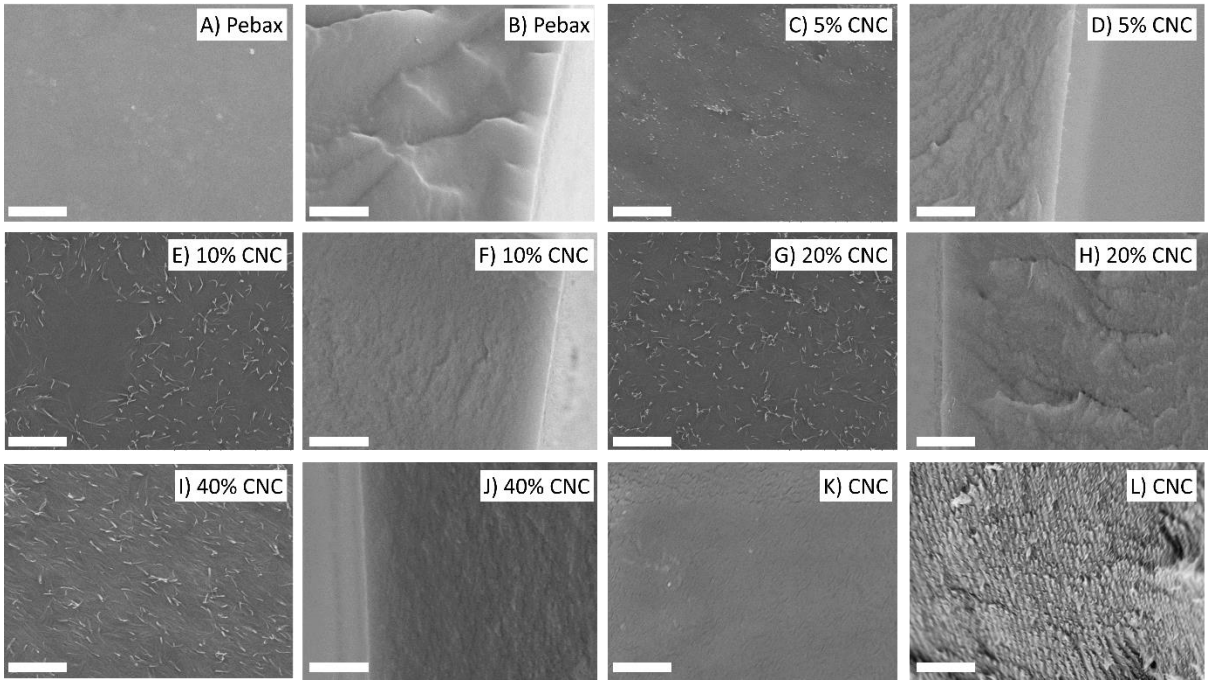

Figure 2. SEM image of: surface (A) and cross-section (B) of neat Pebax, surface (C) and cross-section (D) of 5 wt.% CNC/Pebax, surface (E) and cross-section (F) of 10 wt.% CNC/Pebax, surface (G) and cross-section (H) of 20 wt.% CNC/Pebax, surface (I) and cross-section (J) of 40 wt.% CNC/Pebax, and surface (K) and cross-section (J) of neat CNC. The scale bars in all images represent 5 μm.

The neat Pebax membrane shows both smooth surface and cross-section, typical for a dense polymeric membrane. While in the CNC/Pebax hybrid membranes, it is clearly shown that the CNC is evenly distributed in the Pebax matrix within the studied range. With increasing CNC content, the observed CNC on both surfaces and in the cross-section increases. No obvious phase separation is observed for CNC/Pebax system, even when a CNC content is up to 40 wt.%. However, the tendency of the CNC alignment notably increases with increasing CNC contents, especially that of the 40% CNC sample.

For the pure CNC sample, no individual nanocellulose crystal can be identified from the surface at the same magnification (i.e., 10k) used to observe other membrane samples, but from the cross-section images of the neat CNC film, it is seen that the CNCs were self-assembled and

Postprint:
Zhongde Dai, et al., Industrial & Engineering Chemistry Research, 2022, 61, 25, 9067–9076
https://doi.org/10.1021/acs.iecr.2c01402

formed the regular layered structure, which is in good agreement with the literature.[23, 24] A tendency to form a similar regular structure between CNCs is also found in the membrane with 40% CNC. This layered structure is believed the result of strong hydrogen bonding between CNCs.[25, 26]

3.2 Thermal properties

To investigate the thermal property of the CNC/Pebax hybrid membranes, TGA and DSC tests of the obtained samples were carried out.

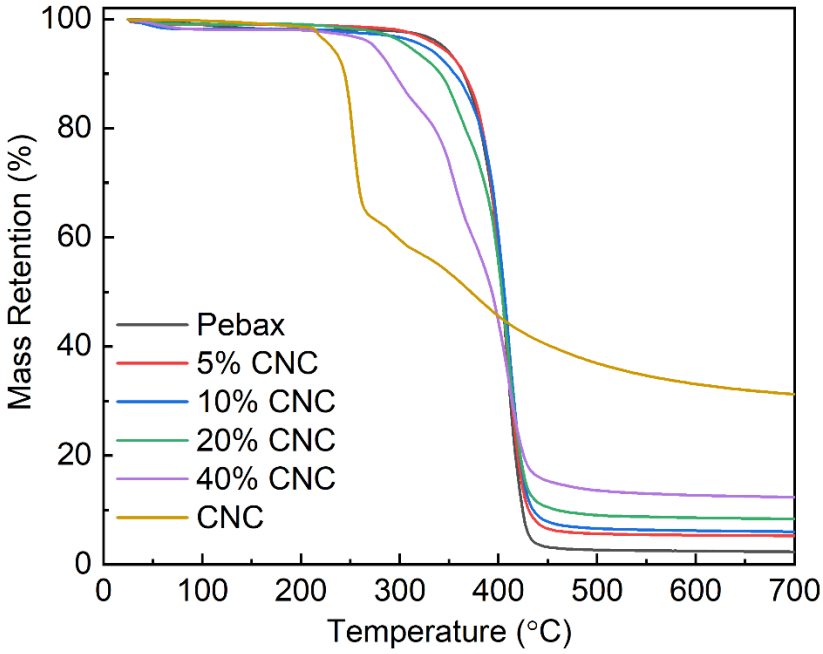

Figure 3. TGA results of the Pebax membrane with different content of CNC.

Figure 3 shows the TGA results of the CNC/Pebax hybrid membranes. Neat Pebax 1657 decomposes in the range of 300 ~ 450 °C with a T_{onset} of around 420 °C, in line with the literature's report[27]. While CNC starts fast decomposition at around 200 °C until 270 °C. Some related studies[28, 29] rationalized this decomposition by the treatments needed in CNC fabrication, such as acid-hydrolysis[29]. Afterward, CNC experiences a slower decomposition until the highest temperature investigated in this work (i.e., 700 °C). In the case of the hybrid membranes, TGA curves of the ones with less than 10 wt.% CNC are similar to the neat Pebax, suggesting that the overall thermal stability of these hybrid membranes is mainly dominated by the Pebax phase. As the CNC content further increases to up 40 wt.%, the T_{onset} of the hybrid material reduces from 420 °C to approximately 320 °C, matching the fact that CNC is less thermal stable than Pebax. Nevertheless, the overall thermal stability of the hybrid still fulfills

Postprint:
Zhongde Dai, et al., Industrial & Engineering Chemistry Research, 2022, 61, 25, 9067–9076
https://doi.org/10.1021/acs.iecr.2c01402

the requirement of most CO_2 separation processes (e.g., post-combustion CO_2, natural gas sweetening, and biogas upgrade), which are generally operated lower than 100 °C.

As temperature rise above 450 °C, Pebax completely decomposes (the residual is less than 3 wt.%), while the residual of CNC still remains 30-40 wt.% of initial mass even at 700 °C, due possibly to forming complex cross-linked or carbon-like structures at high temperature. In terms of the hybrid materials, their residual masses at corresponding temperature (> 450 °C) increase with the CNC content. More interestingly, the residual mass fraction at 700 °C of CNC/Pebax membranes exhibits a nearly linear relationship with the original CNC loading, which indicates the actual CNC contents in the hybrid membranes match with the ones as expected.

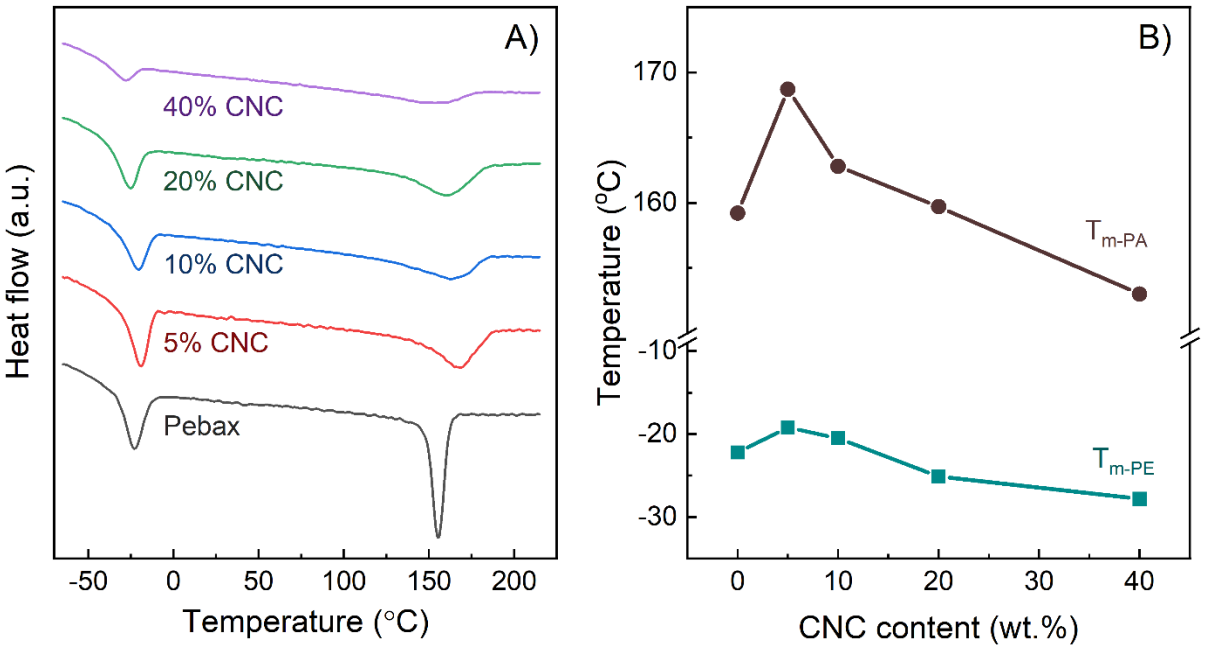

Figure 4. DSC curves of the Pebax membrane with different content of CNC (A), and comparison of melting temperature (T_m) for PE and PI segment in Pebax with different CNC content (B).

The DSC curves from the second cooling scan of CNC/Pebax hybrid membranes are presented in **Figure 4A**. Pebax 1657 has two exothermic peaks, which locates at -40 ~ -10 °C and 150 ~170 °C, respectively, corresponding to the melting temperatures of soft polyether block (T_{m-PE}) and rigid polyamide block (T_{m-PA}).[30] Adding CNC into Pebax affects the melting temperatures of the Pebax matrix: as shown in **Figure 4B**, there exists a maximum for both melting temperatures within the studied CNC loading. It is worth mentioning that, when CNC loading reaches 20 wt% or higher, both T_{m-PE} and T_{m-PA} in the hybrid membranes are lower than those in neat Pebax. The decreased melting temperatures of polymer caused by blending

generally can be ascribed to the increased flexibility of polymer chains, hinting that CNC may work as a physical plasticizer for Pebax 1657 matrix. A similar trend has been also reported in the case of blending POSS into Pebax.[31] Despite the position of $T_{m\text{-}PE}$ being slightly changed; its peak shape was not significantly changed by CNC content. But, the $T_{m\text{-}PA}$ peak of all the hybrid membranes became broader compared to the neat Pebax, with an obvious shoulder presented at the higher temperature. This possibly denotes that the CNC might not be homogeneously mixed into the polyamide domains at higher loadings.[31]

3.3 Fourier-transform infrared spectroscopy (FTIR)

FTIR was used to characterize the CNC/Pebax samples and the results are shown in **Figure 5**. The two representative groups in the Pebax polymer chain, namely the amine and the ketone group, correspond to the peaks at 1657 and 1640 cm^{-1}, respectively, in its FTIR spectrum. The peak at 3300 cm^{-1} can be also assigned to the stretching vibration of N-H.[32] Detailed peak assignment can be seen in **Table 1**.

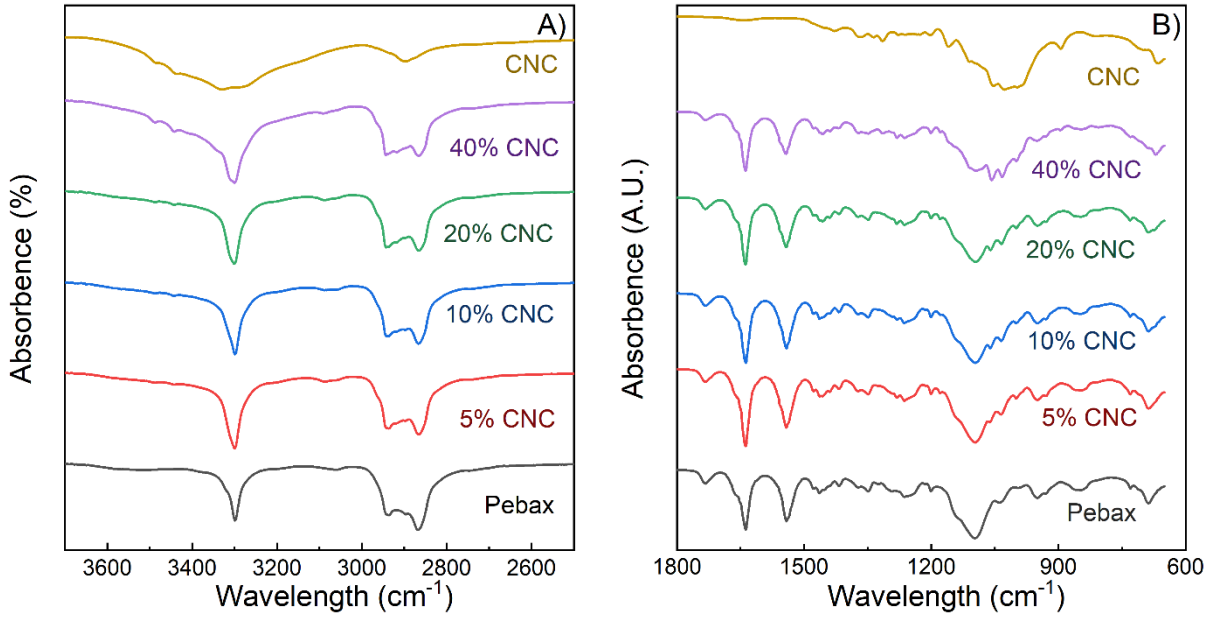

Figure 5. FTIR spectrum of CNC/Pebax hybrid membranes

Table 1. Peak assignment of Pebax and CNC/Pebax membranes

Peak position (cm^{-1})	Peak assignment
844	OH stretching vibration
1090	C–O–C stretching vibration
1640	H–N–C=O
1730	C=O stretching vibration

3300	N–H
2860	CH_3 symmetric stretching vibration
2940	aliphatic -C-H

As the CNC content in the membrane increases, the intensity of representative peaks for Pebax reduces (3300 cm^{-1}), while the corresponding CNC peaks increase (~1030 cm^{-1}). In the entire investigated range, no new peaks or peak position shifts were observed, denoting no chemical interaction between Pebax and CNC exists.

3.4 X-ray Diffraction (XRD)

The crystalline properties of CNC/Pebax hybrid membranes were measured by XRD, and the results are shown in **Figure 6**.

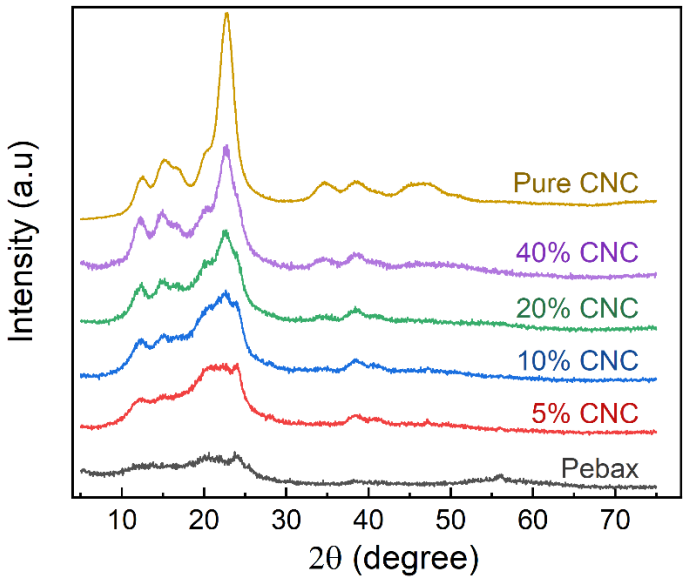

Figure 6. XRD spectra of CNC/Pebax hybrid membranes with different CNC content.

The neat Pebax has wide diffraction peaks at 12°, 24°, and 56° of 2θ[33], and a typical low crystalline nature. The crystalline zones in Pebax1657 are mainly contributed by the polyamide segment, which will display a sharp peak at around 2θ of 21°. However, it is not observed in current work, probably thanking to the relatively thick thickness[34], indicating the low crystallinity of the Pebax phase.

On the contrary, the CNC shows several narrow and sharp peaks in its XRD spectrum, due to its more crystalline nature. Since the Pebax phase shows little crystalline nature, the crystallinity value of CNC phase can provide qualitative information about the overall

crystalline nature of the hybrid materials. Therefore, the crystallinity of the cellulose in hybrid membranes was calculated using the "Segal's method", a commonly used method to calculate the crystallinity index (CI) of cellulose.[35] The CI value of cellulose phase was calculated via equation (3):

$$CI = 100 * \frac{I_{200} - I_{AM}}{I_{200}} \qquad (3)$$

In which I_{200} represents the highest diffraction intensity of the (200) lattice (i.e., 2θ of 22.6°) and corresponds to the amount of crystalline cellulose, I_{AM} is the height of the minimum intensity of the major peaks (i.e., 2θ of 18.4°) and matches the amorphous content of the cellulose.[36] The CI values in hybrid membranes are listed in **Table 2**.

Table 2. Crystallinity value of cellulose phase in CNC/Pebax hybrid membrane with different CNC contents

Material	CI of cellulose phase (%)
5% CNC	33.63
10%CNC	41.97
20% CNC	56.39
40% CNC	64.19
Pure CNC	82.90

As indicated in **Table 2**, for pure CNC, a relatively high CI value (i.e., 82.90%) was obtained, which was comparable with other nanocellulose (e.g., 70%-85%).[36, 37] It has been found that nanocellulose preparation methods, as well as drying conditions, could make significant differences in the crystalline value of the resultant samples,[38] thus in our work, all the hybrid membrane samples were prepared and dried in the same procedure. From **Table 2**, as expected, the CI value increases with the CNC content. Surprisingly, the cellulose crystallinity in membrane (CI value × CNC loading) is concave to the CNC loading axis, and the ideal mixing rule over-estimates the contribution of CNC phase to the overall crystallinity of hybrid membranes. This indicates that less crystalline cellulose existed in CNC phase of the hybrid membrane compared to the neat CNC.

3.5 Mixed gas permeation results

Mixed gas permeation was carried out under dry and fully humid conditions with 10 vol% CO_2 in N_2 as feed, and the results are presented in **Figure 7**.

Postprint:
Zhongde Dai, et al., Industrial & Engineering Chemistry Research, 2022, 61, 25, 9067–9076
https://doi.org/10.1021/acs.iecr.2c01402

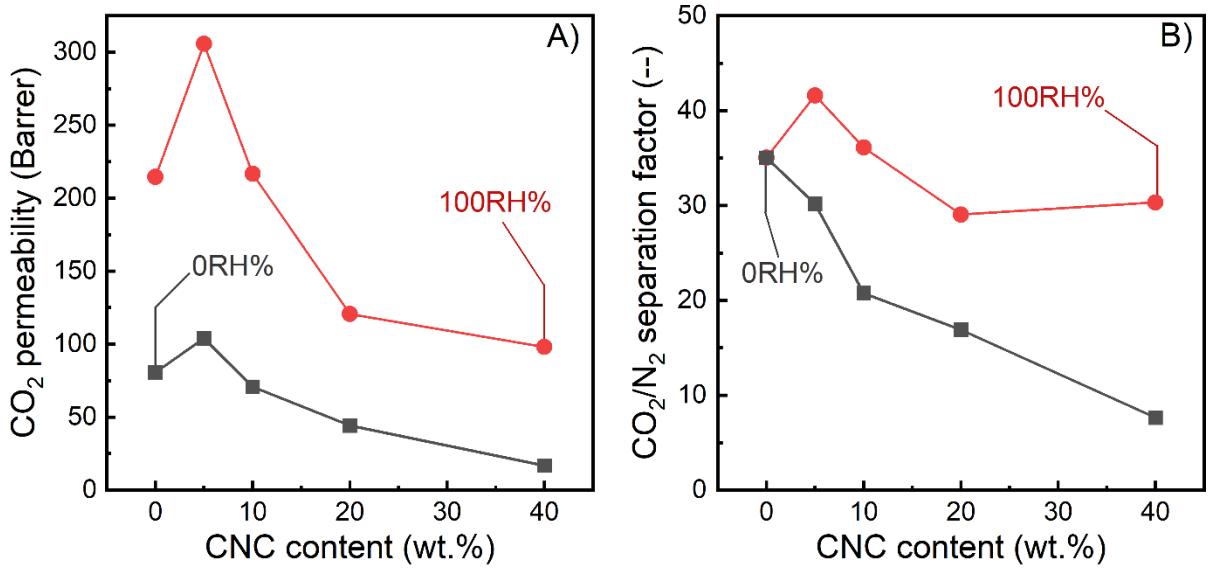

Figure 7. CO_2 permeability (A) and CO_2/N_2 selectivity (B) of CNC/Pebax membranes under dry (0RH%) and fully humid (100RH%) conditions, respectively.

As shown in **Figure 7**, in a dry state, the Pebax membrane presented a moderate CO_2 permeability (80.7 Barrer) and CO_2/N_2 separation factor (35.0), which is comparable with other reported literature.[39-42] Loading only 5 wt% CNC into Pebax matrix resulted in a 29% increased CO_2 permeability (104.0 Barrer), but with slightly reduced selectivity (30.2). Attempts were made to further increase the CNC content in the membrane. However, further increasing CNC content from 10 wt% to 40 wt% resulted in both reduced CO_2 permeability and CO_2/N_2 selectivity.

The gas transport property of CNC-based membranes is largely influenced by humidity. In this work, the CNC/Pebax membrane has been evaluated using fully humid feed gas. As can be seen, increasing the RH value from 0% to 100% results in a sharp increment in CO_2 permeability and CO_2/N_2 selectivity of both neat Pebax and hybrid membranes. For instance, the CO_2 permeability of the neat Pebax increases from 80.7 Barrer to 214.5 Barrer. Similar results have been reported for Pebax membranes in several works.[43, 44] In the case of CNC/Pebax samples, a CO_2 permeability of 305.7 Barrer with a CO_2/N_2 selectivity of 41.6 was observed for the hybrid membranes with 5 wt.% CNC at humid conditions, exhibiting a 42% and 18% improvement, respectively, compared the neat Pebax membrane. However, further increasing the CNC content results in both reduction in CO_2 permeability and CO_2/N_2 selectivity, similar to the gas permeation results obtained from the dry state. Increasing CNC content to 20 wt.% or 40 wt.% even further reduces CO_2 permeability and CO_2/N_2 selectivity, simultaneously.

These results are distinctive from the enhancement observed in CO_2 separation performance of both PVAm/CNC [14] and PVA/nanocellulose,[16] of which the CO_2 permeability increases with CNC loading. A possible explanation of this phenomenon may come from the membrane morphology shown in the SEM image. As can be seen from SEM images (**Figure 2**), at a lower CNC content, the CNC is randomly dispersed in the Pebax matrix. However, as the CNC content increases in the CNC/Pebax hybrid membranes, the CNC tends to form a more orientated alignment, resulting in a much highly packed structure. This alignment of CNC has been widely reported in the literature, and these aligned CNCs can further self-assembly into various complicated hierarchical structures under different conditions[23], which can be beneficial for other applications, but not in this work. Moreover, the XRD results revealed that the CNC phase contains more crystalline zone with increasing CNC amount in membranes. These features limit the gas diffusion and thus the transport through, as noticed in several studies[13, 45], in the CNC/Pebax hybrid membranes. Therefore, it is reasonable to conjecture that at high CNC content, the formation of well-packed highly-crystalline CNC inhibits overall gas transport in the CNC/Pebax hybrid membranes. But at low CNC loading, the abundant hydroxy groups on the CNC surface attract a higher-than-average amount of water near CNC, which facilitates the CO_2 transport. These two transport mechanisms are expressed in **Scheme 2**.

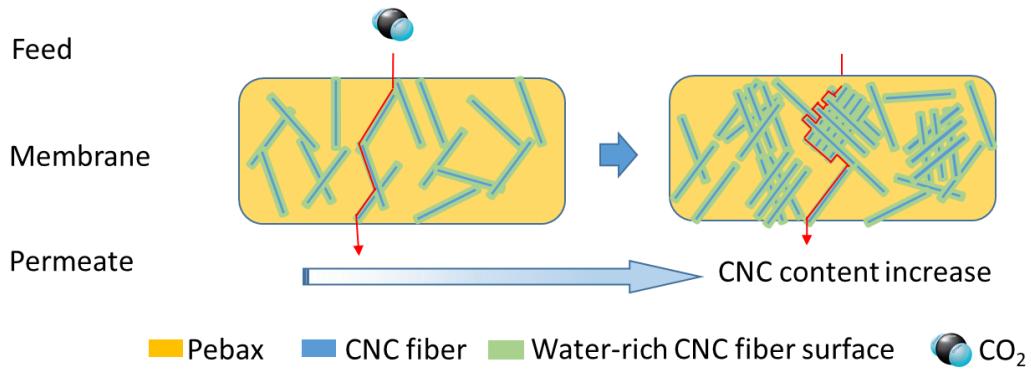

Scheme 2. CO_2 transport in CNC/Pebax hybrid membranes with low (left) and high (right) CNC loading, respectively.

3.6 Comparison of nanocellulose-based membrane separation performances

Some CO_2/N_2 separation results of nanocellulose-based hybrid membranes have been summarized and presented in both **Figure 8** and **Table 3**. Since humidity greatly affects the gas transport in nanocellulose-based materials,[13, 14] most of these membranes were evaluated under humid conditions. Compared to other nanocellulose-based hybrid membranes, CNC/Pebax has relatively high CO_2 permeability with moderate CO_2/N_2 selectivity, especially

compared to the nanocellulose/PVA and nanocellulose/PVAm. This may be explained by the hydrophilicity of the polymer phase, which affects the water amount sorbed by membranes. For example, 1 g of PVAm and PVA can sorb > 1g [14] and 0.75g water,[46] respectively, from a fully saturated gaseous feed. While this value of Pebax 1657 is around 0.2-0.4 g.[47, 48] The lower water concentration in Pebax 1657 membranes limits the swelling degree of nanocellulose, resulting in less improvement in the CO_2 separation performance. Despite this, its CO_2/N_2 separation remains close to Upper Bound 2008, which is still attractive for CO_2/N_2 separation.

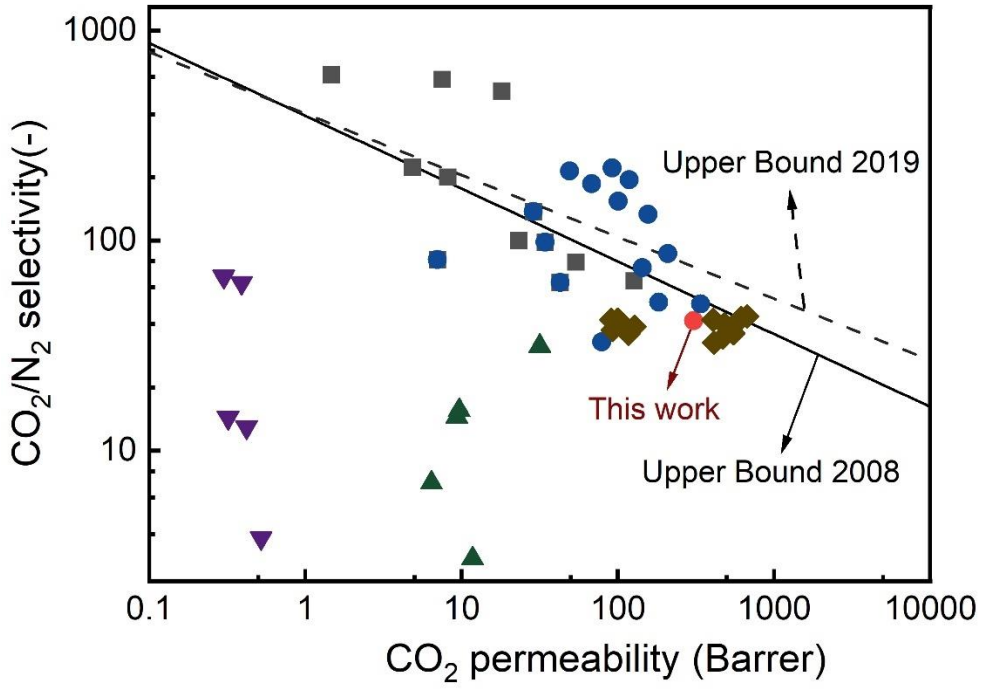

Figure 8. Comparison separation performances of nanocellulose-based hybrid membranes for CO_2/N_2 separation to Upper Bounds.[49, 50] ■: neat nanocellulose self-standing membrane,[13, 14] ●: nanocellulose/PVAm blended membrane,[13, 14, 51] ▲: CNF/polyetherimide (PEI) membrane,[52] ▼: CNF/cellulose acetate (CA) membrane,[52] ♦: nanocellulose/PVA composite membrane.[16, 18, 19]

Table 3. CO_2/N_2 separation performances of the nanocellulose-based membrane.

Membrane	P_{CO2} (Barrer)	$\alpha_{CO2/N2}$ (-)	Test conditions	Refs.
CNF	17.66	515.79	Single gas, 1 bar, 35 °C, 85 RH%	13
CNF	127.07	64.25	Single gas, 1 bar, 35 °C, 80 RH%	14
PVAm+30 wt% CNF	209.16	86.55	Single gas, 1 bar, 35 °C, 80 RH%	14
PVAm+50 wt% CNF	182.86	50.83	Single gas, 1 bar, 35 °C, 90 RH%	13
PVAm+70 wt% CNF	79	32.93	Single gas, 1 bar, 35 °C, 80 RH%	14

27.5 wt.% PVAm + 27.5 wt.% CNC + 45 wt.%Arg	340	50	Single gas, 35 °C, 100 RH%	45
63 wt.% sterically hindered PVAm + 7 wt.% PVA+ 30 wt.% PEG-modified CNF	195.6*	41.3	Mixed gas (10 vol% N_2 in CO_2), 1.7 bar, 35 °C, 100 RH%	51
PEI+0.28 wt% CNF	9.65*	15.57	Single gas, feed: 6.8 bar, permeate: 1 bar	52
PEI + 0.28 wt% bleached CNF	31.69*	31.48		
CA + 0.40 wt% CNF	0.3*	67.38		
CA + 0.29 wt% bleached CNF	0.39*	62.93		
PVA+ 4 wt.% low charged CNC	92.6*	37.5	Mixed gas (10 vol% CO_2 in N_2), 1.2 bar, 23 °C, 95 RH%	18
PVA+ 4 wt.% high charged CNC	90.7*	42		
PVA+ 4wt.% Phosphorylated CNC	100*	42		
PVA+ 4wt.% CNC	128*	39		
PVA+80 wt.% CNC	671.95*	43.6	Mixed gas (10 vol% CO_2 in N_2), 2 bar, R.T., 100 RH%	16
PVA+80 wt.% CNF	470.79*	34.57		
PVA+ 10 wt.% high charged CNF	117	36	Mixed gas (10 vol% CO_2 in N_2), 2 bar, R.T., 100 RH%	19
Pebax 1657+5 wt.% CNC	305.7	41.6	Mixed gas (10 vol% CO_2 in N_2), 2 bar, R.T., 100 RH%	Current study

*: Calculated from permeance; PEG: polyether glycol

4. Conclusion

In the current study, up to 40wt.% CNC was successfully embedded into the Pebax 1657 matrix to fabricate self-standing hybrid membranes. The CNCs are evenly distributed in the polymeric matrix without obvious agglomeration at low CNC loading. While, at high CNC loading, CNCs show self-assembly in hybrid membranes and form an orientated structure, similar to those in neat CNC films. From the thermal property analysis, adding CNC into the Pebax matrix significantly changes the thermal properties of the mixture. The presence of CNC firstly increases both the $T_{m\text{-}PE}$ and $T_{m\text{-}PA}$, denoting the CNC changes the polymeric chain packing in the hybrid membrane. In addition, the T_{onset} of hybrid membranes is over 300 °C, which is much higher than most of the post-combustion CO_2 capture conditions (< 100 °C).

The hybrid membranes were evaluated with significantly improved performance compared with the neat Pebax 1657 membranes. From the mixed gas permeation results, an optimized CNC content exists for both CO_2 permeability and CO_2/N_2 selectivity. Adding only 5 wt.% CNC could effectively improve the CO_2 transport in the hybrid membranes. However, if the CNC content further increases, the regular structure formed by CNC limits CO_2 transport and thus lowers CO_2 permeability. Under optimized conditions, a CO_2 permeability of 305.7 Barrer,

accomplished with a CO_2/N_2 selectivity of 41.6 can be obtained, which are 42% and 18%, respectively, increased compared to the Pebax under the same conditions.

The high performance of the CNC/Pebax hybrid membrane makes it a competitive candidate for CO_2 capture from flue gas. The separation performance of the membrane could be further improved by the functionalization of CNC, such as introducing more CO_2-philic groups onto the CNC surface or a third facilitated transport media (e.g., ionic liquids, amino acid salts) into the hybrid membranes. Given the excellent film-forming properties and compatibility with several commercially available porous substrates, fabricating TFC membranes from the CNC/Pebax hybrid materials is promising. Further optimization of the fabrication and upscaling for this hybrid material into TFC and hollow fiber configuration is ongoing.

Conflicts of interest

There are no conflicts to declare.

Acknowledgments

This work acknowledges the financial support from Sichuan Science and Technology Program (2021YFH0116) and National Natural Science Foundation of China (No. 52170112).

References

1. Anwar, M. N.; Fayyaz, A.; Sohail, N. F.; Khokhar, M. F.; Baqar, M.; Khan, W. D.; Rasool, K.; Rehan, M.; Nizami, A. S., CO_2 capture and storage: A way forward for sustainable environment. *Journal of Environmental Management* **2018,** *226*, 131-144.
2. Fernández, J. R.; Garcia, S.; Sanz-Pérez, E. S., CO_2 Capture and Utilization Editorial. *Industrial & Engineering Chemistry Research* **2020,** *59* (15), 6767-6772.
3. He, X., A review of material development in the field of carbon capture and the application of membrane-based processes in power plants and energy-intensive industries. *Energy, Sustainability and Society* **2018,** *8* (1), 34.
4. Kárászová, M.; Zach, B.; Petrusová, Z.; Červenka, V.; Bobák, M.; Šyc, M.; Izák, P., Post-combustion carbon capture by membrane separation, Review. *Separation and Purification Technology* **2020,** *238*, 116448.
5. Wang, S.; Li, X.; Wu, H.; Tian, Z.; Xin, Q.; He, G.; Peng, D.; Chen, S.; Yin, Y.; Jiang, Z.; Guiver, M. D., Advances in high permeability polymer-based membrane materials for CO_2 separations. *Energy & Environmental Science* **2016,** *9* (6), 1863-1890.
6. Xie, K.; Fu, Q.; Qiao, G. G.; Webley, P. A., Recent progress on fabrication methods of polymeric thin film gas separation membranes for CO_2 capture. *Journal of Membrane Science* **2019,** *572*, 38-60.
7. Guo, M.; Zhang, Y.; Xu, R.; Ren, X.; Huang, W.; Zhong, J.; Tsuru, T.; Kanezashi, M., Ultrahigh permeation of CO_2 capture using composite organosilica membranes. *Separation and Purification Technology* **2022,** *282*, 120061.
8. Demir, H.; Aksu, G. O.; Gulbalkan, H. C.; Keskin, S., MOF Membranes for CO_2 Capture: Past, Present and Future. *Carbon Capture Science & Technology* **2022,** *2*, 100026.

9. Kim, J.-H.; Shim, B. S.; Kim, H. S.; Lee, Y.-J.; Min, S.-K.; Jang, D.; Abas, Z.; Kim, J., Review of nanocellulose for sustainable future materials. *International Journal of Precision Engineering and Manufacturing-Green Technology* **2015,** *2* (2), 197-213.
10. Dai, Z.; Ottesen, V.; Deng, J.; Helberg, R. M. L.; Deng, L., A Brief Review of Nanocellulose Based Hybrid Membranes for CO_2 Separation. *Fibers* **2019,** *7* (5), 40.
11. Wu, Y.; Liang, Y.; Mei, C.; Cai, L.; Nadda, A.; Le, Q. V.; Peng, Y.; Lam, S. S.; Sonne, C.; Xia, C., Advanced nanocellulose-based gas barrier materials: Present status and prospects. *Chemosphere* **2022,** *286*, 131891.
12. Chowdhury, R. A.; Nuruddin, M.; Clarkson, C.; Montes, F.; Howarter, J.; Youngblood, J. P., Cellulose Nanocrystal (CNC) Coatings with Controlled Anisotropy as High-Performance Gas Barrier Films. *ACS Applied Materials & Interfaces* **2019,** *11* (1), 1376-1383.
13. Ansaloni, L.; Salas-Gay, J.; Ligi, S.; Baschetti, M. G., Nanocellulose-based membranes for CO_2 capture. *Journal of Membrane Science* **2017,** *522*, 216-225.
14. Venturi, D.; Grupkovic, D.; Sisti, L.; Baschetti, M. G., Effect of humidity and nanocellulose content on Polyvinylamine-nanocellulose hybrid membranes for CO_2 capture. *Journal of Membrane Science* **2018,** *548*, 263-274.
15. Xu, X.; Liu, F.; Jiang, L.; Zhu, J. Y.; Haagenson, D.; Wiesenborn, D. P., Cellulose Nanocrystals vs. Cellulose Nanofibrils: A Comparative Study on Their Microstructures and Effects as Polymer Reinforcing Agents. *ACS Applied Materials & Interfaces* **2013,** *5* (8), 2999-3009.
16. Dai, Z.; Deng, J.; Yu, Q.; Helberg, R. M. L.; Janakiram, S.; Ansaloni, L.; Deng, L., Fabrication and Evaluation of Bio-Based Nanocomposite TFC Hollow Fiber Membranes for Enhanced CO_2 Capture. *ACS Applied Materials & Interfaces* **2019,** *11* (11), 10874-10882.
17. Jahan, Z.; Niazi, M. B. K.; Hägg, M.-B.; Gregersen, Ø. W., Decoupling the effect of membrane thickness and CNC concentration in PVA based nanocomposite membranes for CO_2/CH_4 separation. *Separation and Purification Technology* **2018,** *204*, 220-225.
18. Torstensen, J. Ø.; Helberg, R. M. L.; Deng, L.; Gregersen, Ø. W.; Syverud, K., PVA/nanocellulose nanocomposite membranes for CO_2 separation from flue gas. *International Journal of Greenhouse Gas Control* **2019,** *81*, 93-102.
19. Helberg, R. M. L.; Torstensen, J. Ø.; Dai, Z.; Janakiram, S.; Chinga-Carrasco, G.; Gregersen, Ø. W.; Syverud, K.; Deng, L., Nanocomposite membranes with high-charge and size-screened phosphorylated nanocellulose fibrils for CO_2 separation. *Green Energy & Environment* **2021,** *6* (4), 585-596.
20. Jahan, Z.; Niazi, M. B. K.; Hagg, M.-B.; Gregersen, Ø. W.; Hussain, A., Phosphorylated nanocellulose fibrils/PVA nanocomposite membranes for biogas upgrading at higher pressure. *Separation Science and Technology* **2020,** *55* (8), 1524-1534.
21. Lin, H.; Thompson, S. M.; Serbanescu-Martin, A.; Wijmans, J. G.; Amo, K. D.; Lokhandwala, K. A.; Low, B. T.; Merkel, T. C., Dehydration of natural gas using membranes. Part II: Sweep/countercurrent design and field test. *Journal of Membrane Science* **2013,** *432*, 106-114.
22. Ahmad, J.; Rehman, W. U.; Deshmukh, K.; Basha, S. K.; Ahamed, B.; Chidambaram, K., Recent Advances in Poly (Amide-B-Ethylene) Based Membranes for Carbon Dioxide (CO2) Capture: A Review. *Polymer-Plastics Technology and Materials* **2019,** *58* (4), 366-383.
23. De France, K.; Zeng, Z.; Wu, T.; Nyström, G., Functional Materials from Nanocellulose: Utilizing Structure–Property Relationships in Bottom-Up Fabrication. *Advanced Materials* **2021,** *33* (28), 2000657.
24. Parker, R. M.; Guidetti, G.; Williams, C. A.; Zhao, T.; Narkevicius, A.; Vignolini, S.; Frka-Petesic, B., The Self-Assembly of Cellulose Nanocrystals: Hierarchical Design of Visual Appearance. *Advanced Materials* **2018,** *30* (19), 1704477.
25. Thomas, B.; Raj, M. C.; B, A. K.; H, R. M.; Joy, J.; Moores, A.; Drisko, G. L.; Sanchez, C., Nanocellulose, a Versatile Green Platform: From Biosources to Materials and Their Applications. *Chemical Reviews* **2018,** *118* (24), 11575-11625.

26. Trache, D.; Tarchoun, A. F.; Derradji, M.; Hamidon, T. S.; Masruchin, N.; Brosse, N.; Hussin, M. H., Nanocellulose: From Fundamentals to Advanced Applications. *Frontiers in Chemistry* **2020,** *8*.
27. Zheng, W.; Ding, R.; Yang, K.; Dai, Y.; Yan, X.; He, G., ZIF-8 nanoparticles with tunable size for enhanced CO_2 capture of Pebax based MMMs. *Separation and Purification Technology* **2019,** *214*, 111-119.
28. Arnata, I. W.; Suprihatin, S.; Fahma, F.; Richana, N.; Sunarti, T. C., Cationic modification of nanocrystalline cellulose from sago fronds. *Cellulose* **2020,** *27* (6), 3121-3141.
29. Kim, D.-Y.; Lee, B.-M.; Koo, D. H.; Kang, P.-H.; Jeun, J.-P., Preparation of nanocellulose from a kenaf core using E-beam irradiation and acid hydrolysis. *Cellulose* **2016,** *23* (5), 3039-3049.
30. Wang, X.; Ding, X.; Zhao, H.; Fu, J.; Xin, Q.; Zhang, Y., Pebax-based mixed matrix membranes containing hollow polypyrrole nanospheres with mesoporous shells for enhanced gas permeation performance. *Journal of Membrane Science* **2020,** *602*, 117968.
31. Rahman, M. M.; Filiz, V.; Shishatskiy, S.; Abetz, C.; Neumann, S.; Bolmer, S.; Khan, M. M.; Abetz, V., PEBAX® with PEG functionalized POSS as nanocomposite membranes for CO_2 separation. *Journal of Membrane Science* **2013,** *437*, 286-297.
32. Zhao, D.; Ren, J.; Li, H.; Li, X.; Deng, M., Gas separation properties of poly(amide-6-b-ethylene oxide)/amino modified multi-walled carbon nanotubes mixed matrix membranes. *Journal of Membrane Science* **2014,** *467*, 41-47.
33. Murali, R. S.; Sridhar, S.; Sankarshana, T.; Ravikumar, Y., Gas permeation behavior of Pebax-1657 nanocomposite membrane incorporated with multiwalled carbon nanotubes. *Industrial & Engineering Chemistry Research* **2010,** *49* (14), 6530-6538.
34. Sharma, P.; Kim, Y.-J.; Kim, M.-Z.; Alam, S. F.; Cho, C. H., A stable polymeric chain configuration producing high performance PEBAX-1657 membranes for CO2 separation. *Nanoscale Advances* **2019,** *1* (7), 2633-2644.
35. Bansal, P.; Hall, M.; Realff, M. J.; Lee, J. H.; Bommarius, A. S., Multivariate statistical analysis of X-ray data from cellulose: A new method to determine degree of crystallinity and predict hydrolysis rates. *Bioresource Technology* **2010,** *101* (12), 4461-4471.
36. Santmartí, A.; Lee, K.-Y. J. N.; sustainability: Production, p., applications,; studies, c., Crystallinity and thermal stability of nanocellulose. **2018**, 67-86.
37. Nang An, V.; Chi Nhan, H. T.; Tap, T. D.; Van, T. T. T.; Van Viet, P.; Van Hieu, L., Extraction of High Crystalline Nanocellulose from Biorenewable Sources of Vietnamese Agricultural Wastes. *Journal of Polymers and the Environment* **2020,** *28* (5), 1465-1474.
38. Peng, Y.; Gardner, D. J.; Han, Y.; Kiziltas, A.; Cai, Z.; Tshabalala, M. A., Influence of drying method on the material properties of nanocellulose I: thermostability and crystallinity. *Cellulose* **2013,** *20* (5), 2379-2392.
39. Deng, J.; Dai, Z.; Hou, J.; Deng, L., Morphologically tunable MOF nanosheets in mixed matrix membranes for CO_2 separation. *Chemistry of Materials* **2020,** *32* (10), 4174-4184.
40. Dai, Z.; Deng, J.; Peng, K.-J.; Liu, Y.-L.; Deng, L., Pebax/PEG Grafted CNT Hybrid Membranes for Enhanced CO_2/N_2 Separation. *Industrial & Engineering Chemistry Research* **2019,** *58* (27), 12226-12234.
41. Li, T.; Pan, Y.; Peinemann, K.-V.; Lai, Z., Carbon dioxide selective mixed matrix composite membrane containing ZIF-7 nano-fillers. *Journal of Membrane Science* **2013,** *425-426*, 235-242.
42. Car, A.; Stropnik, C.; Yave, W.; Peinemann, K.-V., PEG modified poly(amide-b-ethylene oxide) membranes for CO_2 separation. *Journal of Membrane Science* **2008,** *307* (1), 88-95.
43. Xiang, L.; Pan, Y.; Zeng, G.; Jiang, J.; Chen, J.; Wang, C., Preparation of poly(ether-block-amide)/attapulgite mixed matrix membranes for CO_2/N_2 separation. *Journal of Membrane Science* **2016,** *500*, 66-75.
44. Shishatskiy, S.; Pauls, J. R.; Nunes, S. P.; Peinemann, K.-V., Quaternary ammonium membrane materials for CO_2 separation. *Journal of Membrane Science* **2010,** *359* (1), 44-53.

45. Casadei, R.; Firouznia, E.; Baschetti, M. G., Effect of Mobile Carrier on the Performance of PVAm–Nanocellulose Facilitated Transport Membranes for CO_2 Capture. *Membranes* **2021,** *11* (6), 442.
46. Deng, L.; Hägg, M.-B., Swelling behavior and gas permeation performance of PVAm/PVA blend FSC membrane. *Journal of Membrane Science* **2010,** *363* (1), 295-301.
47. Sridhar, S.; Suryamurali, R.; Smitha, B.; Aminabhavi, T. M., Development of crosslinked poly(ether-block-amide) membrane for CO_2/CH_4 separation. *Colloids and Surfaces A: Physicochemical and Engineering Aspects* **2007,** *297* (1), 267-274.
48. Thanakkasaranee, S.; Kim, D.; Seo, J., Preparation and Characterization of Poly(ether-block-amide)/Polyethylene Glycol Composite Films with Temperature-Dependent Permeation. *Polymers (Basel)* **2018,** *10* (2).
49. Robeson, L. M., The upper bound revisited. *Journal of Membrane Science* **2008,** *320* (1), 390-400.
50. Comesaña-Gándara, B.; Chen, J.; Bezzu, C. G.; Carta, M.; Rose, I.; Ferrari, M.-C.; Esposito, E.; Fuoco, A.; Jansen, J. C.; McKeown, N. B., Redefining the Robeson upper bounds for CO_2/CH_4 and CO_2/N_2 separations using a series of ultrapermeable benzotriptycene-based polymers of intrinsic microporosity. *Energy & Environmental Science* **2019,** *12* (9), 2733-2740.
51. Janakiram, S.; Yu, X.; Ansaloni, L.; Dai, Z.; Deng, L., Manipulation of Fibril Surfaces in Nanocellulose-Based Facilitated Transport Membranes for Enhanced CO_2 Capture. *ACS Applied Materials & Interfaces* **2019,** *11* (36), 33302-33313.
52. Uribe, H. A. Effects of Bark Derived Nanocellulose on Gas Separation Membranes. M.A.S., University of Toronto, Ann Arbor, 2018.